

The Mechanics of Conceptual Interpretation in GPT Models: Interpretative Insights

Nura Aljaafari^{1,4†}, Danilo S. Carvalho^{1,3}, André Freitas^{1,2,3}

¹ Department of Computer Science, University of Manchester, United Kingdom

² Idiap Research Institute, Switzerland

³ National Biomarker Centre, CRUK-MI, Univ. of Manchester, United Kingdom

⁴ King Faisal University, Al Hofuf, KSA

{firstname.lastname}@[postgrad.]manchester.ac.uk

Abstract

Locating and editing knowledge in large language models (LLMs) is crucial for enhancing their accuracy, safety, and inference rationale. We introduce “concept editing”, an innovative variation of knowledge editing that uncovers conceptualisation mechanisms within these models. Using the reverse dictionary task, inference tracing, and input abstraction, we analyse the Multi-Layer Perceptron (MLP), Multi-Head Attention (MHA), and hidden state components of transformer models. Our results reveal distinct patterns: MLP layers employ key-value retrieval mechanism and context-dependent processing, which are highly associated with relative input tokens. MHA layers demonstrate a distributed nature with significant higher-level activations, suggesting sophisticated semantic integration. Hidden states emphasise the importance of the last token and top layers in the inference process. We observe evidence of gradual information building and distributed representation. These observations elucidate how transformer models process semantic information, paving the way for targeted interventions and improved interpretability techniques. Our work highlights the complex, layered nature of semantic processing in LLMs and the challenges of isolating and modifying specific concepts within these models.

1 Introduction

The interpretation and reasoning over concepts are integral to natural language (NL) understanding tasks such as textual entailment and question answering. Language models (LMs) are assumed to perform conceptual interpretation, but this is often evaluated extrinsically on proxy tasks, with limited literature elucidating how LMs represent and interpret concepts.

Conceptual interpretation, a subset of semantic interpretation, involves mapping lexical items and structures to concepts, i.e., abstract notions of entities, events, quantities, and rules (Brown, 2006;

Hirst, 1987). This mapping is fundamental to language learning and use, grounding its capability to transmit information through interactions with the observable world.

Research on transformer-based large language models (LLMs) has established that these models represent factual associations as localisable network activation patterns (Geva et al., 2021; Dai et al., 2022), enabling the development of efficient approaches to update targeted associations, known as *knowledge editing* (Dai et al., 2022; Meng et al., 2022).

However, locating and updating modelled factual associations does not determine whether these associations are based on valid interpretations of the corresponding concepts. Thus, characterising interpretation mechanisms is necessary for effective explainability and validation of LM capabilities.

Challenges in characterising conceptual interpretation mechanisms in LMs include (i) defining an interpretation task simple enough to evaluate conceptual interpretation in isolation and (ii) establishing an intervention to observe the internal representation of a language model during inference.

Efforts to abstract representations by reverse-engineering network activations, such as *Mechanistic Interpretability*, allow for fine-grained LLM analysis but are limited in scalability. We propose uncovering interpretation mechanisms at a higher granularity by leveraging linguistic signals (e.g., argument structure, semantic roles) to perform symbolic extraction of the compositional patterns involved in factual associations. Specifically, we examine *natural language definitions* as a baseline for isolating conceptual interpretation and their corresponding structural and semantic signals. Having the localisation of concept composition as a means of interpretation.

To elucidate how transformer-based LMs interpret concepts, we introduce *concept editing*, a variation of knowledge editing defined over the *reverse dic-*

tionary definition generation task. This method uses causal tracing and Rank-One Model Editing (ROME) (Meng et al., 2022) to localise internal projection and decision states within generative LMs.

This paper focuses on the following overarching research questions: “What are the observable representation patterns that characterise conceptual interpretation within LMs?” and “Can we localise specialised representational patterns to derive an interpretation model within LMs?”.

In order to answer these research questions, this paper provides the following contributions:

1. Introduction of the task of concept editing, a variation of knowledge editing, grounded in the reverse dictionary definition generation task.
2. An extensive systematic analysis of the representation components within a transformer (Multi-Layer Perceptron (MLP) layers, Multi-Head Attention (MHA) layers and hidden states) across different target languages.
3. Eliciting of a conceptual interpretation model for LMs based on the observed representation patterns.

Empirical analysis indicates that compositionality is critical in observed representation patterns. Models do not process a concept through a single, direct mapping of a definition to its definiendum. Instead, different model components (MLP layers, MHA layers, and hidden states) interact and complement each other to form a conceptual understanding, each utilising different aspects of the input tokens. This process involves MLP layers focusing on specific lexical and semantic features, while MHA layers and hidden states aggregate broader contextual information to reach a final representation of the concept.

In the following sections, we present: (2) relevant background knowledge; (3) the proposed approach in detail; (4) empirical analysis and discussion; (5) related work; (6) conclusion; and (7, and 8) final remarks.

2 NL Definitions & Concept Representation

Natural language definitions. In this work, we use NL definitions as the foundational linguistic artefact to elucidate conceptual interpretation in

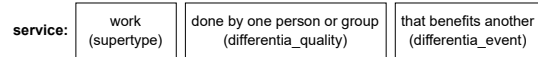


Figure 1: Example of definitional semantic labelling for the term service.

transformer-based LMs. Although NL definitions do not capture the complete picture of conceptual representation, they provide a contained setting to evaluate conceptual compositionality. Dictionary-style NL definitions offer a concise expression (“definiens”) of the *necessary and sufficient conditions* (NSC) and essential attributes of a defined term (“definiendum”). Interpreting definition statements (definiendum + definiens) requires syntax interpretation, disambiguation, and meaning composition of tokens/words, which are common to all sentence-level interpretation tasks.

We emphasise the intensional (set-theoretical) descriptive aspect of definitions, which gives meaning to a term by specifying NSC for its use. For example, the term “odd” can be defined as “numerically indivisible by two”, describing a condition that is both necessary (a number must fulfil it to be odd) and sufficient (any number that fulfils it is considered odd). Intensional definitions also include a *genus-differentia* type of structure (Silva et al., 2016), describing meanings in terms of a genus (a broader associated set) and differentia (terms that further specialise the genus set). For instance, the term “service” can be defined as “work done by one person or group that benefits another”, with “work” as its genus and the remainder as its differentia (Figure 1).

Conceptual composition. We examine composition from a Montagovian perspective, where the meaning of a compound expression is a function of the meanings of its parts and their syntactic combination (Partee et al., 1984). This perspective is chosen under the consideration that pragmatics need to be solved at the LM context window level. Thus, we define the sentence representation model based on Argument Structure Theory (AST) and the thematic roles associated with definitional statements (Silva et al., 2016).

AST (Jackendoff, 1992; Levin, 1993; Rappaport Hovav and Levin, 2008) represents sentence structure and meaning in terms of the interface between syntactic structure and the semantic roles of arguments. It delineates how verbs define the organisation of their arguments and reflect this organisation in syntactic realisation. AST abstracts

sentences as predicate-argument structures, where the predicate p (associated with the verb) has a set of associated arguments arg_i , each with a positional component i and a thematic/semantic role r_i , categorising the definitional semantic functions of arguments (e.g., genus, differentia-qualia) (see Table 1 in Appendix B.1 for all roles and their description). In this work, the AST predicate-argument representation is linked to a lexical-semantic representation of the content c_i of the term t_i .

Following (Silva et al., 2016), we define the composition between argument types and modifier phenomena for each argument, where the structural syntactic/semantic relationship is defined by its shallow semantics. This composition involves the content of the terms, their position in the predicate-argument (PArg) structure (arg_i), and their definitional semantic roles (DSRs) (r_i : *pred*, *arg*). Formally, a definiens statement $s_{definiens}$ consists of a sequence of PArgs/SRs and word content associations. Upon encoding in latent space, this can be described as:

$$[[s_{definiens}]] = \underbrace{t_1(c_1, r_1)}_{\text{i.e., ARG0-genus}} \oplus \dots \oplus \underbrace{t_i(c_i, r_i)}_{\text{ARGN-differentia-quality}} \quad (1)$$

where $[[s_{definiendum}]] = [[s_{definiens}]]$ and $t_i(c_i, r_i) = c_i \otimes r_i$ represents the semantics of term t_i with content c_i (i.e., *animals*) and DSR r_i (i.e., *ARG0-genus*) in context s , \otimes : connects the meanings of words with their roles, using the compositional-distributional semantics notation of (Smolensky and Legendre, 2006; Clark et al., 2008). \oplus : connects the lexical semantics (word content + structural role) to form the definition semantics.

Reverse dictionary task. A valid formal interpretation of a definition involves attributing a meaning to each symbol in the definiens so that it evaluates it as true for any valid use of the definiendum. In NL, this process is analogous to the *reverse dictionary* task: selecting the correct dictionary term given a definition sentence. This task can serve as a proxy for measuring interpretation quality in a given domain. For generative LMs, this is typically framed as a next-token prediction task, where the definition sentence is the prompt and the definiendum is the expected answer. The interpretation of the definiens can be extended to form the following hypothesis: if an LM’s predictions are accurate, showing high proxy interpretation quality, the model can assign correct meanings to all prompted symbols. The LM achieves this by capturing the concep-

tual and compositional structure of the definiens and operating over them through its internal representations. Validating this hypothesis can provide insights into the relationship between a model’s internal representations and a formalised notion of interpretation for NL, bridging linguistic and statistical efforts in the interpretability analysis of LMs.

Knowledge editing & localisation in LLMs. Identifying concept representation patterns within LMs is crucial for updating the models’ knowledge. These patterns, expressed as activation patterns, encapsulate the internal representations of concepts. Therefore, recognising these patterns would give us the ability to efficiently control and edit the knowledge captured by LMs.

Recent studies such as Knowledge Neurons (Dai et al., 2022) and ROME (Meng et al., 2022) have focused on handling *factual information* in LMs to modify individual facts by targeting these specific activation patterns. Methods like MEMIT (Meng et al., 2023) and PMET (Li et al., 2024) build on the aforementioned approaches and enhance their capability to update batches of information simultaneously.

This work examines several mechanisms that could be involved in the conceptual interpretation of LMs, elucidating how these models process and comprehend meaning. We prioritise five mechanisms in this study. We investigate and extend the Key-Value Representation Mechanism (KVRM) to examine concept storage and retrieval in MLP layers. We study the Token Integration Mechanism (TIM) in early-layers. We track Gradual Information Aggregation to understand the evolution of concepts within the model. We explore neuron polysemanticity to gain insights into the mapping of multiple concepts to one component in the model. Finally, we investigate the Distributed Representation Mechanism (DRM) to uncover how a concept is encoded across several parts of the model.

KVRM concerns the storage and retrieval of factual information in a key-value pair format, as explored by Geva et al. (2021) and Dai et al. (2022). This process involves the Feed-Forward Network (FFN) of the MLP component (Equation 5), where the first layer processes the input to generate an activation pattern (key), the second layer retrieves corresponding representations (value) that represent this key. This mechanism helps identify and locate specific concept representations within the model, and we argue that if a concept is not di-

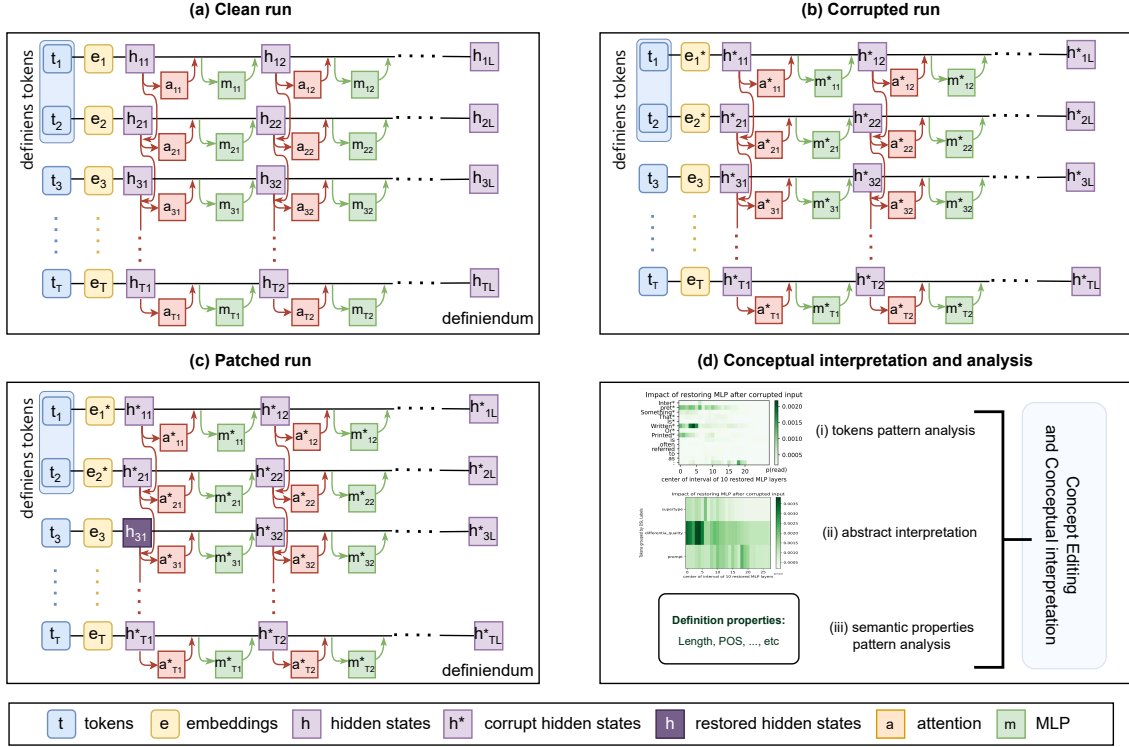


Figure 2: Overview of causal tracing and conceptual locating in LMs.

rectly mapped, then it is inferred. TIM describes the de-/re-tokenisation process hypothesised by Elhage et al. (2022a), which occurs in early neurons that group split words into their original form and meaning. Gradual information aggregation refers to layers acting as integrative functions, specifically, combining basic features produced in the early layers with more complex features in the upper layers. Studies, including Krzyzanowski et al. (2024), have shown that in smaller models like GPT-2 small, early layers handle shallow syntactic features while later layers encode more complex concepts. Neuron polysemanticity is the phenomenon where multiple, unrelated concepts activate a neuron (Elhage et al., 2022b). DRM, a foundational notion in neural networks, involves encoding a concept across multiple neurons, each capturing different aspects of the data (Hinton et al., 1986).

We argue that DRM is inherent in LLMs and examine how other mechanisms contribute to conceptual interpretation. Our hypothesis suggests that MLP layers demonstrate specialised behaviours in obtaining and encoding input tokens, whereas other components of the model support and enhance them. Our objective is to expand current

techniques and utilise established patterns to identify conceptual interpretation and construction in LLMs. This methodology would enable us to investigate how LLMs acquire and improve their understanding of thematic roles, offering valuable information about their functional specialisation and hierarchical processing.

3 Proposed Approach

3.1 Localisation via Causal tracing

This work defines a variation of the ROME method (Meng et al., 2022), employing its *causal tracing* approach to elicit supporting representation patterns. Figure 2 illustrates the causal tracing along with our conceptual interpretation approach, with (a-c) inspired by (Meng et al., 2022).

We assume a transformer model \mathcal{M} with L layers processing an input of length T , structured as a tuple $\langle (definiens, prompt, definiendum) \rangle$, where the definiens part is of length N .

Following (Vaswani et al., 2017), in transformer models, individual tokens (t) engage in attention mechanisms with preceding states across other tokens. Each layer’s representation (h_t^l) integrates global multi head attention ($MHA_t^{(l)}$) and MLP

($MLP_t^{(l)}$) from preceding layers into the current layer l , alongside the preceding states’ hidden representations. This mechanism is formulated as:

$$h_t^l = h_t^{(l-1)} + MHA_t^l + MLP_t^l \quad (2)$$

where,

$$MHA_t^l = Concat_{h=1}^H(MHA^{l,h}(h_{\leq t}^{(l-1)})) \quad (3)$$

let,

$$h_t^{mid,l} = LayerNorm(h_t^{l-1} + MHA_t^l) \quad (4)$$

then,

$$\begin{aligned} MLP_t^l &= FFN(h_t^{mid,l}) \\ &= W_2^l \delta(W_1^l \eta(h_t^{mid,l})) \end{aligned} \quad (5)$$

where δ and η are non-linear functions, and FFN represents a feed-forward network.

The causal tracing (also known as activation patching) involves processing the input through the model and recording all hidden MHA and MLP states for all tokens $t \in T$. The initial model output, $\mathcal{M}(X)$, represents the model’s prediction based on the original input.

Next, it introduces corruption to the definiens of length N by adding noise (α) to a subset of token embeddings, sampled from a Gaussian distribution $\mathcal{N}(0, \beta)$, where β is three times the standard deviation of the embeddings. This yields corrupted embeddings $\{e_i^*\}_{i=1}^N$, where $e_i^* = e_i + \alpha$. The corrupted input results in an altered model output $\mathcal{M}^*(X)$, processed through the model while storing all its states.

Finally, a restoration phase is initiated where a subset of the hidden, MHA, or MLP corrupted states are reinstated to their original states from $\mathcal{M}(X)$. The model’s ability to recover the correct prediction during this phase indicates that the restored states encapsulate the most informative representational components.

We refer to the states captured from the initial run and the corruption run as “**clean run**” states and “**corrupted run**” states, respectively, as named in the original paper (Meng et al., 2022).

3.2 Eliciting the conceptual interpretation model

Within causal tracing, the representation of a transformer can be abstracted/simplified as a 2nd order

tensor \mathbf{T}_{ij} , where i corresponds to the input positional dimension, and j corresponds to the layer position index. Given the input tuple $d = \langle (definiens, prompt, definiendum) \rangle$, a causal tracing operator $op(d)$ will return a representation map \mathbf{T}_{ij} where each value of \mathbf{T} is within the normalised range $[0, 1]$. We call the instantiated \mathbf{T} ($[[\mathbf{T}]]$) an *interpretation trace* of d .

Given $[[\mathbf{T}]]$, the intent is to relate to the abstract interpretation model $[[s_{definiens}]]$. The structure of $[[s_{definiens}]]$ provides a categorical probe to interpret $[[\mathbf{T}]]$ regarding the positional component i , enriching it with the argument structure arg_n and associated thematic role Θ .

In this context, we articulate the following RQs, which will drive the experimental design.

RQ1: Are there consistent localisable/observable patterns within $[[\mathbf{T}]]$? Are these patterns consistent across languages?

RQ2: Are there observable specialisation differences in $[[\mathbf{T}]]$ across $k=[MHA, MLP, hidden]$?

To answer RQs 1 and 2, we define conceptual localisation probes. Given a set of reverse dictionary generation tuples D_l and a set of interpretation traces $[[\mathbf{T}_{ijl}]]$, each map serves as a visual and positional probe highlighting the necessary and critical states for the model to achieve the correct prediction. While this type of probe provides a coarse-grained aggregation of the expressive set of high-dimensional subspaces induced within an LM, we hypothesise that conceptual editing can outline systemic interpretation patterns within the transformer architecture.

RQ3: Can $[[\mathbf{T}]]$ be correlated to the abstract interpretation pattern of $[[s_{definiens}]]$?

To provide an abstraction layer over the definition space, we overlay categories of abstraction which encode syntactic and semantic phenomena, namely Part-of-Speech (POS) and thematic roles (Θ). These categories, alongside the token position and the layer position, allow for the computation of correlations \mathbf{T}_{ij} with these categorical structures.

RQ4: Is there an observable emerging mechanism which describes the conceptual interpretation (as a synthesis of $[[\mathbf{T}]]$ and $[[s_{definiens}]]$)?

4 Empirical Analysis

4.1 Selected Datasets & Models

We generate datasets from WordNet (Miller, 1994) and Spanish WordNet (Gonzalez-Agirre et al.,

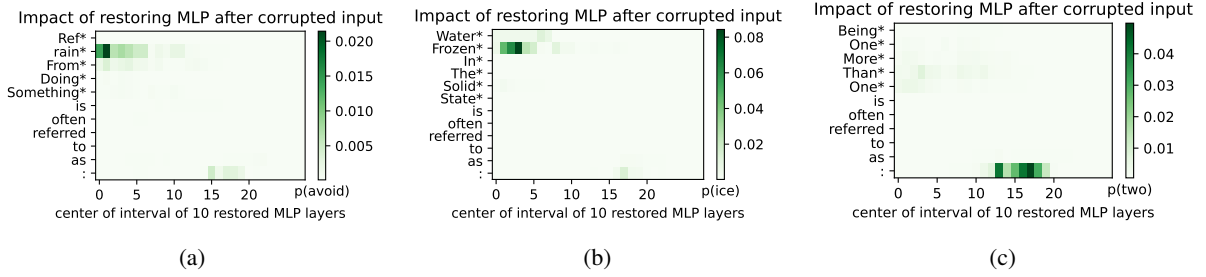


Figure 3: (a-c) Causal traces for GPT-J-6B, illustrating the impact of restoring a window of 10 MLP layers. In all cases, the span of importance is short. The state representation differs between definitions, with strong word content associations in (a) and (b) and weaker content associations in (c).

2012), referred to as English WordNet (EWN) and Spanish WordNet (SWN), for this study. The datasets contain annotated pairs $\{(c_i, d_i)\}_{i=1}^N$, where each pair consists of a definition and a definiendum. EWN has 8348 samples (80/20 train-test split), and SWN has 7815 samples (30/70 train-test split) (see Appendix A for detailed dataset creation and filtering processes). Each sample in EWN was augmented with Definitional Semantic Roles (DSR) labels (Silva et al., 2016), for aiding in answering RQ3.¹

The models used are GPT-J-6B (Wang and Komatsuzaki, 2021) and BERTIN GPT-J-6B (la Rosa and Fernández, 2022), both with 6 billion parameters, obtained from Hugging Face, and fine-tuned via Low-Rank Adaptation (LoRA) (Hu et al., 2021) and Quantized LoRA (Dettmers et al., 2024). Prompts with the highest accuracy were chosen as query prompts (see Appendix A.3 for a detailed prompt selection process). The analysis was limited to the test definitions that were predicted correctly by fine-tuned models. GPT-J-6B and BERTIN GPT-J-6B were chosen for their accessibility, performance, manageable size for knowledge editing, and multi-language availability. Datasets and source code are available for reproducibility at [< anonymisedlink >](#).

4.2 Localisation of conceptual interpretation patterns

Figures 3, 7 and 10 follow the same visualisation approach as described in (Meng et al., 2022). The y-axis (top to bottom) represents the input tokens to the model, where an asterisk added to the token indicates added noise. The x-axis shows the layer number from the first to the last layer (represented from 0 to $L - 1$), moving from left to

¹DSR annotations were limited to EWN due to their unavailability for the Spanish dataset.

right. Each cell in the heatmap denotes the value associated with the impact of restoring a particular state (derived from the clean run at the token’s location), indicating the model’s regained ability to accurately predict the correct label. A greater intensity (values are normalised [0,1]) indicates a higher level of contribution to the prediction of the definiendum.

Figures 4, 8 and 11 represent the top 10 states in a component. The x-axis shows the layer index, and the y-axis indicates occurrences in the top values. The dark lines are smoothed interpolations for clearer trend analysis.

To report results statically, we segmented input tokens into pre-prompt (i.e., the definition tokens divided in half into early and mid tokens) and prompt tokens and analysed their top 10 and 50 states. We also aggregated the tracing results by normalising them to a uniform shape, which allowed us to report general trends in each model component. To do this, we sampled roughly 80% of the data with inputs of similar length and then appended the shorter ones with zeros to unify their sizes. The samples were aggregated to their mean and median, referred to as the mean and median causal traces.

4.2.1 MLP: Content association, lexical signalling and adaptive behaviour.

The analysis of MLP layers reveals specific concept formation and manipulation behaviour. Namely, early layers predominantly focus on surface-level lexical tokens, while higher layers engage in more abstract processing.

Early layers exhibit high importance for tokens lexically or semantically related to the definiendum (Figures 3a and 3b), **forming what we term “Basis Concepts”—fundamental semantic units directly derived from input tokens.** Activation importance *shifts* to the last tokens in higher layers

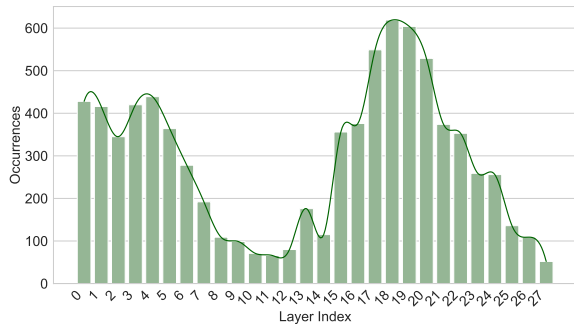


Figure 4: Distribution of layer indices in the top 10 locations across 818 samples in the MLP layers. It follows a bimodal pattern with two clusters: the first grouping the early layers and the second grouping the top layers.

when definition tokens lack direct connections to the definiendum (Figure 3c). This shift suggests the formation of **“Emergent Concepts”—concepts that arise from the integration and transformation of Basis Concepts through more complex, context-dependent processing.**

Evidence supports the existence of the Token Integration Mechanism (*TIM*) (explained in Section 2), where early processing of split tokens is done to restore their compositional meaning (Figures 3a, 13a and 13b). The concentration of decisions within a few states supports the hypothesis that MLP layers utilise *KVRM* (presented in Section 2). The observations of *TIM* and the concentrations of activation importance indicate observable and localisable patterns in MLP layers, addressing **RQ1**. A preliminary affirmative response to **RQ2** is also provided by the observed behaviour and the *KVRM* storage method, which point to specialisation variations within model components.

Further distribution analysis of the top 10 states across MLP layers shows that influential activations clustered in the early and upper layers (Figure 4). Layers 17, 18, and 19 accounted for 15%, 17%, and 16% of occurrences, respectively, while lower layers such as 0, 3, and 4 also showed significant activity, each around 12%. Comparing this with the MHA and hidden layer patterns (Figures 8 and 11), we find that important states are primarily in mid-to-top layers, **indicating functional specialisation by layer type and depth**, providing a positive response to **RQ2**. This difference can be attributed to early MLP layers extracting basic concepts, while MHA and hidden layers integrate these concepts into refined representations (emergent concepts).

To analyse the correlation between model behaviour and semantic roles, we grouped activation values according to their definitional semantic roles (DSR). For a full description of the method, we refer the reader to (Silva et al., 2016). Our results (Figures 5a and 5b) show that *supertype* and *differentia_quality* are prominent categories, with activation levels depending on the specificity of the content word. For example, the term “edge”, defined as “the boundary of a surface”, has the highest activation for the *supertype* “boundary”, capturing the highest specificity token in the definition (Figure 5a). We further analysed the statistical distribution of the DSR labels in the top 10 and top 50 states. In the top 10 states, the *prompt* label appeared in around 70% of the top states, followed by *differentia_quality*, with more than 11%, and *supertype* with more than 8%. For the top 50 states, the *prompt* dropped to roughly 49%, while *differentia_quality* jumped to 31.38%, followed by *differentia_event* and *supertype*, which appeared around 6.73% and 6.22%, respectively. This observation aligns with **RQ3**, showing that **the model can identify discriminative semantic features correlating with correct predictions**. Additionally, the importance of single labels spans several consecutive layers (Figure 5); we interpret this as **evidence of information persistence, where crucial semantic features are preserved and processed across multiple layers**. Investigating the impact of definiendum POS reveals consistent model behaviour across various POS (Figure 6), **implying general uniformity in behaviour regardless of definiendum type**. This finding challenges the assumption that different concept types (e.g., nouns, verbs, and adjectives) would necessitate special processing pathways within the model. The observed uniformity denotes an abstract semantic representation level that surpasses traditional grammatical categories for concept formation in LMs (see Appendix D.3 for elaborated results on POS differences).

The aggregation results reveal a concentration of median trace activations in the higher layers (15-22) for the top 10 states, accounting for 70% of the cases, and in the early layers (6-7) for the remaining cases. The mean trace indicates a similar pattern, with a notable concentration of 80% in the higher layers (17-21) and 20% in the early layers (13-14). For the top 50 states, the median trace showed that early layers (0-7) appeared the most with around 50% of the times, while higher lay-

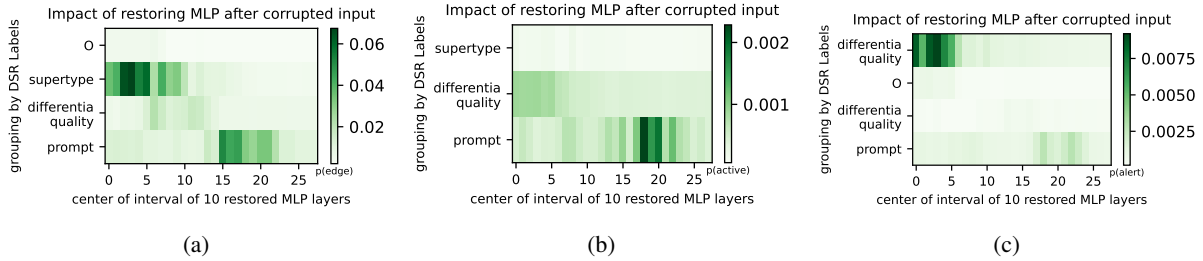


Figure 5: Sample of causal tracing with DSR labelling when restoring a window of 10 MLP layers. The representation highlights the distribution of important states over several layers and the importance of content words, mainly captured in supertype (a) and differentia quality (b) and (c).

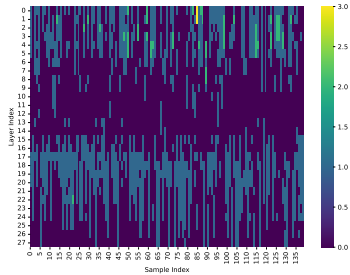
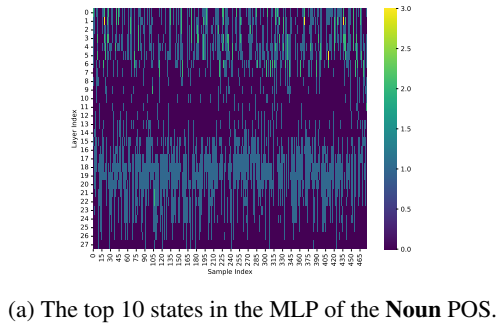


Figure 6: Sample of the top 10 states of the MLP layer grouped based on POS of the definiendum.

ers (15–24) were lower, at 40%. The mean trace shows 56% of important states in the higher layers (17-24) and 22% in the early layers (11-12). **These results show that MLP layers exhibit a variation in representation and spread across layers within specific ranges, highlighting MLP’s non-systematic and polysemantic nature.**

Synthesis: Distinct functional stratification within MLP layers is highlighted by our findings, with lower layers focusing on basic semantic processing and higher layers handling complex concept integration. The absence of strong semantic-indicating tokens is compensated by the composition of content tokens, resulting in two activation clusters that operate both coordinately and complementarily. This structured approach not only enhances the understanding of conceptual inference but also

suggests specialised processing capabilities across LMs.

4.2.2 MHA layers: Compositional-distributional function

The analysis of MHA layers demonstrates two key patterns. First, the last token functions as a representation aggregator prior to generating the final prediction, appearing around 99% in the top 10 important states and 78% in the 50. Second, a wider range of important states is observed compared to MLP layers (Figure 7). These findings align conceptual interpretation with previous studies on factual information extraction (Da et al., 2021) and **suggest a distributed representation of semantic information** compatible with gradual information aggregation and the DRM (mechanisms described in Section 2). Additionally, they illustrate a localisable behaviour within the MHA, addressing **RQ1**. This localisable behaviour aligns with (Voita et al., 2019), who reported that only a subset of MHA heads are crucial for inference, signifying that limited elements within MHA hold significant importance for conceptual interpretation.

DSR labelling analysis of MHA layers supports the hypothesis that **they have a higher aggregation/compositional nature, and semantic specialisation compared to MLP layers** (Figures 5 and 9). The first is reinforced by the concentrations of important states in the middle-upper layers and prompt tokens, consequently forming emergent concepts (Figure 9). The shorter spans of important activations in DSR groups accentuate the second point (Figure 9). Statistically, *prompt* overwhelmingly dominated the top states, appearing at approximately 98% and 54% when sampling the top 10 and 50 states, respectively. Other labels, such as *associated_fact*, *origin_location*, and *purpose*, were less frequent, each accounting for less than 1% of the top 10 states. How-

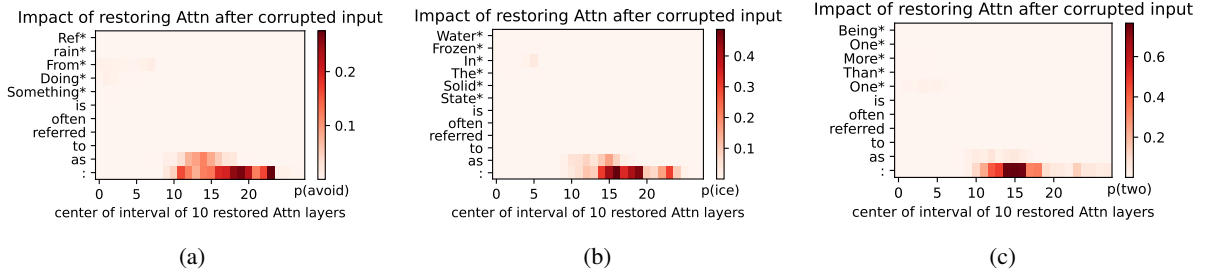


Figure 7: (a-c) Causal traces for GPT-J-6B, illustrating the impact of restoring a window of 10 MHA layers. The important states in all cases are spread and centred in the middle-upper layers, with high associations towards the end of the prompt.

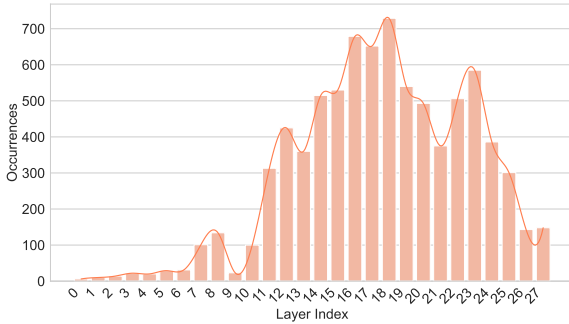


Figure 8: Distribution of layer indices in the top 10 locations across 818 samples in the MHA layers. The distribution mostly follows a unimodal, negatively skewed pattern, showing the concentration of important states in the middle-upper part of the model.

ever, in the top 50 states, these labels increased, with *differentia_quality* rising to over 34% and *differentia_event* exceeding 7%, while others increased but remained at smaller percentages. The differences between the MHA and MLP layers address **RQ2** and highlight the assumed correlation between $[[T]]$ and abstract interpretation in **RQ3**. We notice that MHA layers exhibit dynamic activation patterns **sensitive to small semantic differences in input** (Figures 9a and 9b). **This adaptability indicates a complex distributed representation system where semantic information is dynamically encoded and reconfigured across multiple layers because of contextual differences.** The analysis of 10 significant activation values showed that the most significant states are usually located in the middle-top part of the model (Figure 8), specifically, layers 16, 17 and 18 accounting for 22%, 20%, and 19% of occurrences in the top 10 states, and layers (12-18) account for roughly 25% in the top 50 states, **supporting gradual information building and more complex, emergent semantic processing in MHA’s higher layers.**

The top 10 states for both median and mean traces were all correlated to the last token and centred between layers 15-25 and 17-25. For the top 50 median states, 60% were in higher layers (15-27), while 10% were in mid-layers (11-14). It also shows a 56% concentration in the top layers (15-27), and 28% in the middle layers (12-14). The trend indicated that the layers of **MHA show mixed consistency and variation, have a central cluster, and include a range of values in their broader aggregation.**

Synthesis: The MHA layers display four notable characteristics: (i) important states are distributed and become concentrated through abstraction; (ii) these states are positioned in the middle-upper layers; (iii) they are consistently detectable in the last token; and (iv) processing adapts to small semantic differences in input. These characteristics emphasise MHA layers’ role in LMs’ conceptualisation process, which is done by integrating distributed features and transitioning from basic to emergent concepts; their dynamic, context-sensitive encoding aligns with neuron polysemanticity and DRM mechanisms, showing their versatility and calling for further elicitation of these component mechanisms.

4.2.3 Hidden states: pivotal influence of top Layers and last tokens

The examination of hidden states displays a significant influence of the last token and top layers in the conceptual interpretation process. For example, sampling the top 10 states shows that layers between 21 and 28 accounted for over 85% of occurrences. In the same sample, *prompt* tokens dominate, appearing in 99% of cases. Other locations have negligible percentages in the top 10 states but range between 27% and 18% for early and mid locations when sampling the top 50 states. While

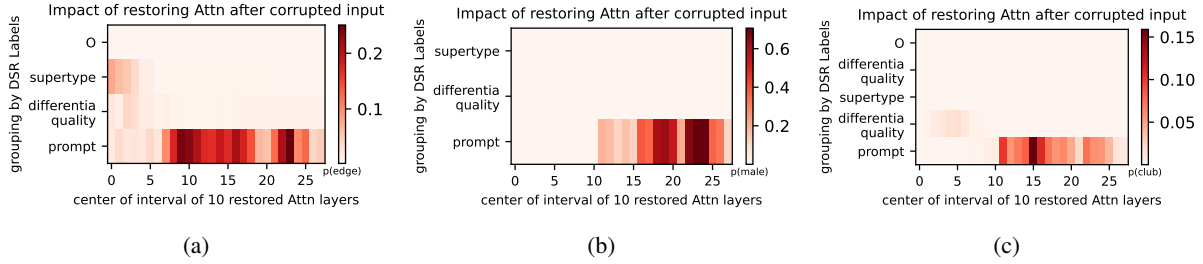


Figure 9: Sample of causal tracing with DSR labelling when restoring a window of 10 MHA layers. The figure illustrates a significant span of important states, mainly linked with the prompt. It also highlights faint clusters of states related to supertype and differentia quality labels, showing their importance in the MHA layers.

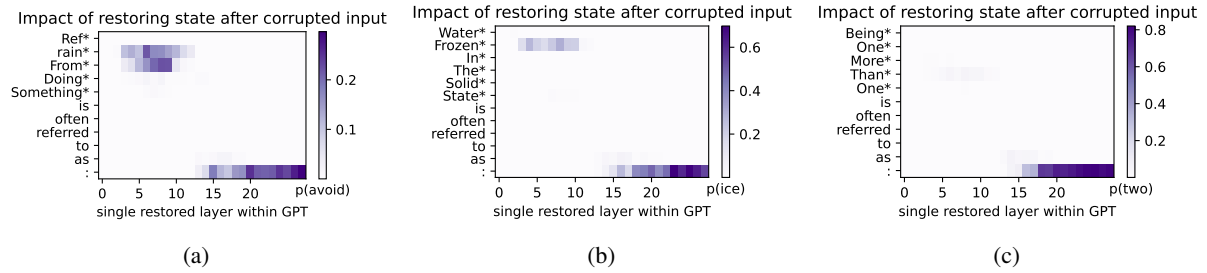


Figure 10: (a-c) Causal traces for GPT-J-6B, illustrating the impact of restoring a hidden state. The important states are predominantly linked with the top layers and the last token; in (a) and (b), other content words have important states but with fewer concentrations.

tokens other than the prompt generally have minimal impact, those related to the definiendum—such as synonyms (Figure 10a) or descriptive modifiers (Figure 10b)—can slightly alter the pattern of important states. Nevertheless, the overall behaviour of the hidden states is consistent, **highlighting a targeted approach where critical elements are emphasised at the end of input processing**. Similar findings were reported in the literature on the specialised role of upper layers in NLP mod-

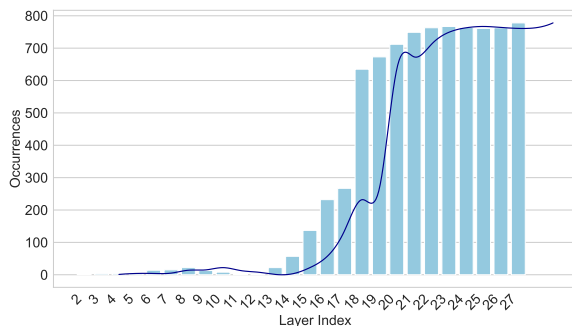


Figure 11: Distribution of layer indices in the top 10 locations across 818 samples in the hidden states. The distribution exhibits a clearly unimodal, negatively skewed pattern, indicating the concentration of important states in the upper part of the model.

els for accurate output predictions, as in (Li et al., 2022) and (Krzyzanowski et al., 2024), providing a strong foundation for our current work. The aforementioned influence is detectable in general causal tracing (Figure 10), causal tracing while applying DSR labelling (Figure 12) and the analysis of the top 10 states (Figure 11).

Since this behaviour was observed in MLP, MHA and hidden states, **we conclude that the gradual information integrative mechanism is present in all [[T]] components**, albeit in varying degrees. The recognition of these patterns answers **RQ1** positively, and these small differences between the components provide a positive response to **RQ2**.

As for applying **DSR labelling** (Figure 12), it is clear that the predictions heavily depend on the same patterns as the general causal tracing, emphasising their role across different contexts and tracing methods. Notably, *differentia_quality* or *differentia_event* were the labels associated with the other few important states. Similar to MHA, *prompt* was the most prominent label, appearing in roughly 99% of the top 10 states and 51% in the top 50 states. Other states were mostly undetectable in the top 10 states, but in the 50 states, we have *differentia_quality* and *differentia_event* accounting for 32% and 7%,

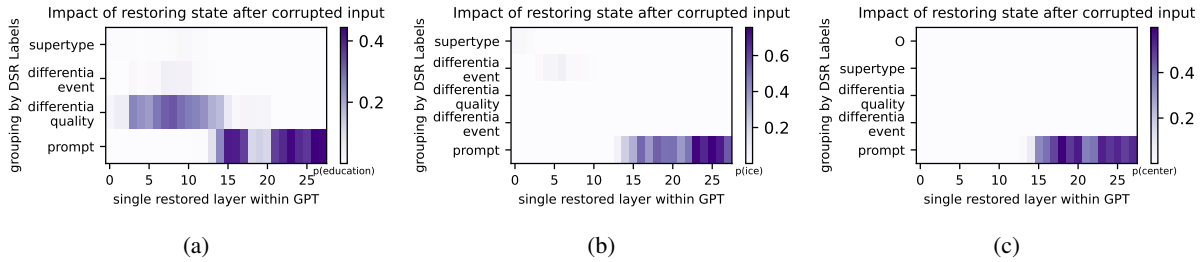


Figure 12: Sample of causal tracing with DSR labelling when restoring a hidden state. In (a), an apparent importance is associated with differential quality. In all (a-c), the important states are distributed in the top layers, and the prompt is linked to these states.

respectively. This analysis of DSR and hidden states serves as a means of addressing **RQ3**, showing how these elements impact the model’s understanding of concepts.

Both the median and mean causal traces show **consistent patterns of hidden states**, with important states clustering around layers 18 to 27, accounting for 100% of the top 10 states. In the top 50, the median trace had 48% of the important states in the higher layers (15-27), 28% in the early layers (0-7), and 24% in the mid-layers (8-14). The mean trace had a comparable distribution, with 54% found in the higher layers (15-27), 36% in the mid-layers (17-24), and 10% in the lower layers (16-18).

Synthesis: Hidden states analysis discloses the following: (i) significant influence of the last token and top layers; (ii) high similarity in terms of behaviour to the MHA layers; and (iii) contextual adaptation through minimal but significant impact of content tokens. These observations demonstrate a hierarchical processing approach in hidden states that predominantly uses the MHA mechanism while being concentrated at the top of the model.

4.3 Results validation

4.3.1 Alternative definitions

To validate our results, we tested the model using “alternative definitions” generated via ChatGPT (OpenAI, 2023). For each sample in the test set, five alternatives were generated, with the condition that each alternative has a high semantic similarity to the original one. The model correctly predicted about 42% of these definitions. These correctly predicted definitions were used to assess the resemblance between their processing and the original definitions. The analysis showed similar patterns across different definitions. The main insights are discussed next.

MLP Layers. Their general patterns were similar (Figure 13), but the same concept is associated with different locations, indicating DRM presence and high susceptibility to variation in input representation. Also, different concepts are mapped to the same location, validating the existence of polysemanticity.

MHA Layers. Patterns for them (Figure 14) were consistent across different definitions of the same concept, suggesting an ability to capture general semantic features regardless of wording.

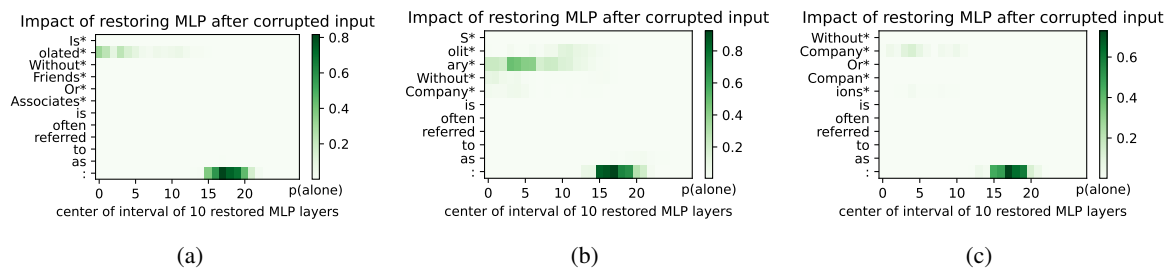


Figure 13: (a-c) Causal traces for GPT-J-6B, illustrating the impact of restoring a window of 10 MLP states for alternative definitions of the same definiendum. Semantically similar words, such as “Isolated” in (a), “Solitary” in (b), and “Without company” in (c), show similar activation patterns, with the concentration captured in the first similar word in each definition. Generally, (a-c) demonstrate a consistent activation pattern across alternative definitions.

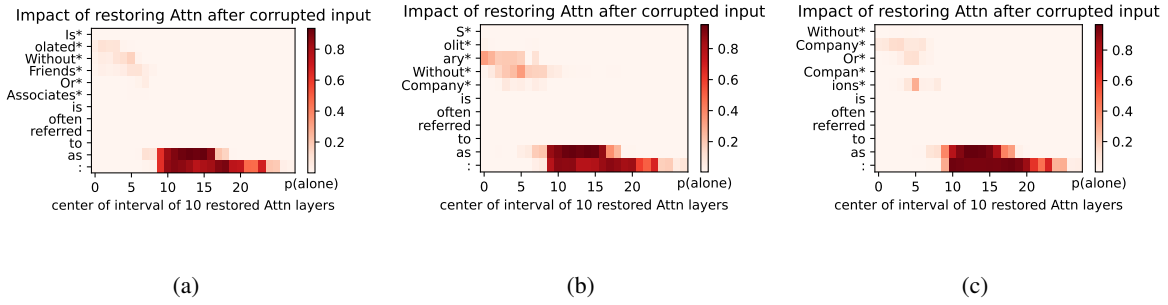


Figure 14: (a-c) Causal traces for GPT-J-6B, illustrating the impact of restoring a window of 10 MHA layers for alternative definitions of the same definiendum. The most important states are linked to prompt tokens and almost mirror each other in (a-c). Other important states in (a-c), mostly linked to content words, show slight differences in activation patterns.

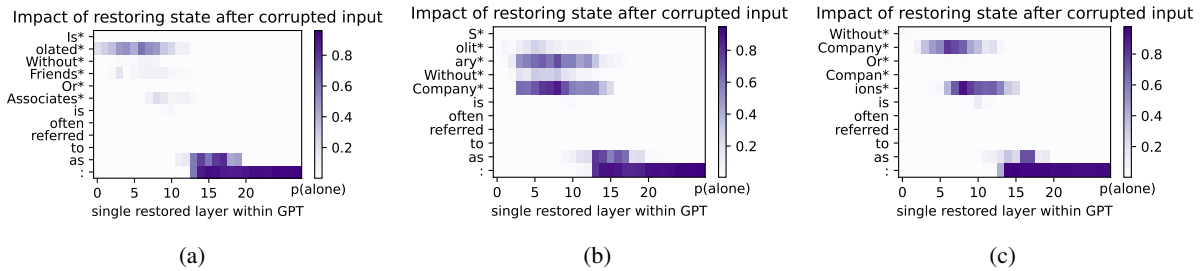


Figure 15: (a-c) Causal traces for GPT-J-6B, illustrating the impact of restoring a hidden state for alternative definitions of the same definiendum. Activation patterns are comparable in all cases (a-c), with semantically similar words, “Isolated” in (a), “Solitary” and “Without company” in (b), and “Without company” and “companions” in (c), exhibiting similar activation patterns.

Hidden States. They tend to focus on similar lexical components, regardless of token positions across definitions (Figure 15). This indicates that hidden layers can identify and prioritise key semantic elements independently of their position. To conclude, these findings confirm the importance of compositionality, and that **the model does not deduce a concept directly** but uses a collaborative process among MLPs, MHA layers, and hidden states, highlighting the complex interplay within the model’s components.

4.3.2 Results are transferable to other models and languages

The operations conducted on EWN and GPT-J-6B were also carried out on SWN and BERTIN GPT-J-6B models. These experiments tested our results’ generalisability across languages, and the main findings are detailed below.

MLP Layers. Spanish tracing patterns mirror those observed in English data, with states in earlier layers being more pronounced, especially towards the end of the definition (Figure 16). Important states are concentrated within one or two key states, but distributed over a slightly broader range of lay-

ers compared to the English results (Figure 16c), indicating subtle processing differences.

MHA Layers. These layers exhibit similar behaviour to English results, with important states associated with the last token and spreading around the top layers (Figure 17).

Hidden States. Consistent patterns were found across both models, with top states found in the last token and top layers (Figure 18). High-importance states in definitions linked to the definiendum were also observed (Figures 18b and 18c).

The hidden states and MHA layers activation patterns are very similar to the ones obtained for English, **indicating a language-agnostic processing mechanism in LMs**. This similarity underscores these components’ abilities to process input based on the semantics of the definition, agnostically to the language the input is presented in, and directly addresses **RQ1** regarding the presence and consistency of localisable/observable patterns within $[[T]]$.

In summary, we notice small differences in patterns associated with concepts between the MLPs between languages, which can be attributed to variations in the formulation or linguistic structure of

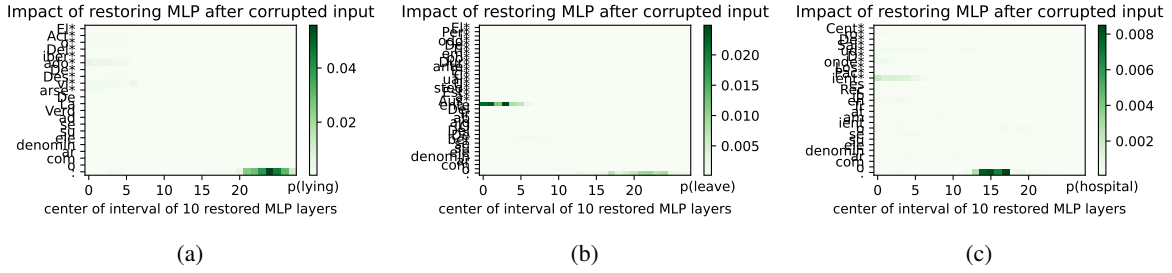


Figure 16: (a-c) Causal traces for BERTIN GPT-J-6B, illustrating the impact of restoring a window of 10 MLP states. In (a) and (b), the important states are around the last token with high intensity for one or two layers. In (c), the significant states are tied with several content tokens spanning several layers with varying intensity depending on token specificity.

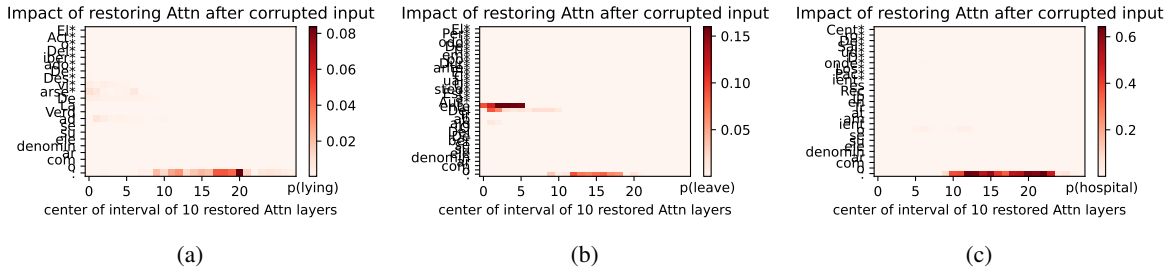


Figure 17: (a-c) Causal traces for BERTIN GPT-J-6B, illustrating the impact of restoring a window of 10 MHA layers. The top states in (a-c) are associated with the last token, with a mostly long span of associated layers, as seen in (b) and (c), but with different intensity patterns.

Spanish definitions compared to English definitions. Our findings indicate that despite being fine-tuned in different languages, the models behave similarly with effective representation of semantic relationships between the definiendum and definition tokens. These findings suggest that models embed semantic information during their input processing rather than depending upon non-semantic or structural properties alone.

4.4 Outline of a conceptual interpretation mechanism in LMs

We present a conceptual interpretation method for LMs to address **RQ4**. The method combines causal

analysis and abstraction for interpreting LMs at a coarse-grained level. We find that models’ components learn and store knowledge distinctly: MLPs learn in a nonsystematic way, following the poly-semantic nature described in the literature (Black et al., 2022) and aligning with our observations of the DRM in MLPs. MHA layers display a formalised inference approach that is language-invariant with consistent conceptual patterns across the different definitions, supporting their role in capturing general semantics. Hidden states aggregate information hierarchically into the upper layers and last tokens.

Based on these findings, we propose that the de-

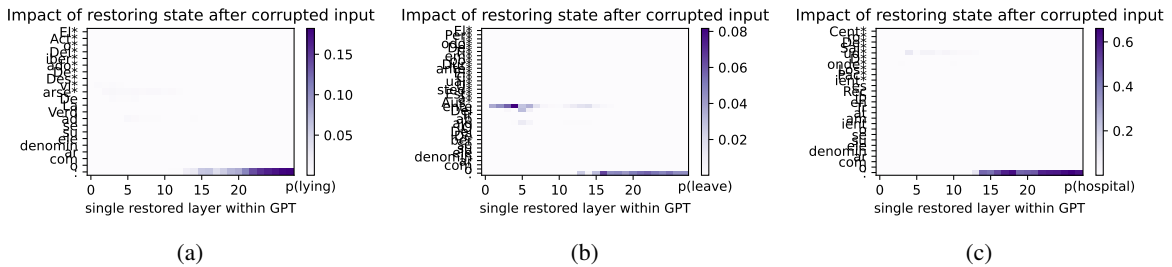


Figure 18: (a-c) Causal traces for BERTIN GPT-J-6B, illustrating the impact of restoring a hidden state. The patterns are consistent across the figures, with (b) and (c) showing other tokens capturing important states with low intensity but having a long-running effect.

sign of conceptual interventions should focus on the input states in (i) early-central MLP layers, (ii) middle-top MHA layers, or (iii) final hidden states. We also propose two avenues for enhancing LMs’ interpretability approaches. First, the causal relationships between MLPs, MHA, and hidden states should be explored for a deeper understanding of information integration and aggregation between layers and components to represent concepts. Second, combining data abstraction with more detailed model tracing (e.g., concentrating on head-level analysis in MHA) to uncover more detailed insights into the model’s functioning.

4.5 Experimental Setup

In all experiments, the NVIDIA RTX A6000 GPU was used for accelerated computation. The Torch deep learning framework version 2.2.2+cu121 was employed for model training and evaluation. Pre-trained language models were leveraged using Hugging Face Transformers version 4.39.3. The experiments were conducted using Python 3.11.7.

5 Related Work

The significant success of Language Models (LMs) across various applications has sparked a keen interest in unravelling their mechanisms, internal representations, and conceptualisation processes (Chung et al., 2023; Touvron et al., 2023)). While mechanistic and conceptual interpretability are intertwined aspects of understanding LMs, it remains challenging to identify a comprehensive approach that seamlessly integrates these two perspectives. **Mechanistic interpretability (MI)** seeks to deconstruct neural networks into programs that can be understood by humans (Conmy et al., 2023). Conceptual interpretation is to identify patterns or abstract representations that underlie the process of inference.

Activation patching, i.e., causal tracing, is an MI technique that selectively modifies and restores sets of activations within LMs throughout the inference process (Heimersheim and Nanda, 2024). ROME (Meng et al., 2022) and MEMIT (Meng et al., 2023) exemplify this method. Causal Scrubbing (Chan et al., 2022) and Attribution Patching (Nanda, 2023) provide improved and efficient activation patching solutions.

Logit attribution methods link model predictions to input tokens using logit values associated with each token (Belrose et al., 2023; Elhage et al.,

2021). A prime example of direct logit attribution is direct logit attribution, introduced by Wang et al. (2022), which was used to study FFN in Geva et al. (2022) and MHA in Ferrando et al. (2023). All the studies yielded significant and informative findings.

Circuit analysis searches for subgraphs, known as circuits, in LMs with defined functions or roles in the models’ functionality (Olsson et al., 2022). Many methods have been proposed for circuit detection, including methods based on activation patching (Wang et al., 2022; Conmy et al., 2023), gradient-approximation (Sarti et al., 2023), and differentiable weight masking (Bayazit et al., 2023). Activation patching provides a more direct and localised method for understanding how specific activations influence LMs’ behaviour than logit attribution and circuit analysis. However, current methodologies frequently concentrate on specific elements of model functionality or highly specialised tasks, potentially overlooking broader concept formation and representation mechanisms. Our work aims to bridge this gap by combining activation patching with abstraction to provide a more thorough approach to understanding conceptual interpretation in LLMs across different model components and languages.

6 Conclusion

The paper gives insights into the process of conceptual interpretation in LMs, focusing on semantic representations across the models’ components. A pivotal factor of our approach was applying definitional semantic labelling that provided abstraction to input tokens, consequently improving the mechanistic elucidation of LMs. For the model components, we found that MLPs exhibit specialised and polysemantic behaviour, MHA layers demonstrate consistent compositional patterns in semantic processing, and hidden states show a gradual aggregation across these specialised components. These insights highlight the existence of systematic conceptualisation within LMs, but we also stress the need for finer interpretability methods. Future work should focus on: developing finer analysis techniques, such as targeting attention heads rather than layers, a deeper exploration the underlying emerging abstractions, and the investigation of causal relationships between model components. This work is aimed to be a stepping stone to finding stronger evidence of LMs mechanisms for concep-

tualisation, thus providing a higher understanding of conceptual semantic processing in LMs across languages and tasks.

7 Ethical Considerations

In our study, we implemented conceptual editing that uses WordNet, abstract labelling, and causal tracing to gain an understanding of the conceptual interpretation mechanisms of transformer-based models. Using WordNet comes with some unintentional risks, such as biases inherent in the dataset. Abstract labelling might result in distorted representations. Conceptual editing has identified mechanisms that can be employed to intentionally alter the behaviour of models in an adverse way. We offer open access to our code and dataset, enabling the research community to easily replicate and verify our work.

8 Limitations

The study has some limitations including: (i) the use of a limited set of autoregressive transformer models within a certain model scale. We focus on sentence-level meaning and single-token prediction tasks, which do not fully reflect the complexities of conceptualisation across other tasks. The analysis mostly targets each component individually rather than investigating causal relationships between them, and MHA was studied as a whole rather than individual heads. Valuable insights may have been overlooked as we selected inference tracing as a target method. These limitations provide context for interpreting our results and highlight areas for future research.

References

- Deniz Bayazit, Negar Foroutan, Zeming Chen, Gail Weiss, and Antoine Bosselut. 2023. Discovering knowledge-critical subnetworks in pretrained language models. *arXiv preprint arXiv:2310.03084*.
- Nora Belrose, Zach Furman, Logan Smith, Danny Hallowi, Igor Ostrovsky, Lev McKinney, Stella Biderman, and Jacob Steinhardt. 2023. Eliciting latent predictions from transformers with the tuned lens. *arXiv preprint arXiv:2303.08112*.
- Sid Black, Lee Sharkey, Leo Grinsztajn, Eric Winsor, Dan Braun, Jacob Merizian, Kip Parker, Carlos Ramón Guevara, Beren Millidge, Gabriel Alfour, et al. 2022. Interpreting neural networks through the polytope lens. *arXiv preprint arXiv:2211.12312*.
- Keith Brown. 2006. *Encyclopedia of language and linguistics (2nd Edition)*, volume 1. Elsevier.
- Lawrence Chan, Adria Garriga-Alonso, Nicholas Goldowsky-Dill, Ryan Greenblatt, Jenny Nitishinskaya, Ansh Radhakrishnan, Buck Shlegeris, and Nate Thomas. 2022. Causal scrubbing: A method for rigorously testing interpretability hypotheses. In *AI Alignment Forum*, pages 1828–1843.
- John Chung, Ece Kamar, and Saleema Amershi. 2023. [Increasing diversity while maintaining accuracy: Text data generation with large language models and human interventions](#). In *Proceedings of the 61st Annual Meeting of the Association for Computational Linguistics (Volume 1: Long Papers)*, pages 575–593, Toronto, Canada. Association for Computational Linguistics.
- Stephen Clark, Bob Coecke, and Mehrnoosh Sadrzadeh. 2008. A compositional distributional model of meaning. In *Proceedings of the Second Quantum Interaction Symposium (QI-2008)*, pages 133–140. Oxford.
- Arthur Conmy, Augustine Mavor-Parker, Aengus Lynch, Stefan Heimersheim, and Adrià Garriga-Alonso. 2023. Towards automated circuit discovery for mechanistic interpretability. *Advances in Neural Information Processing Systems*, 36:16318–16352.
- Jeff Da, Ronan Le Bras, Ximing Lu, Yejin Choi, and Antoine Bosselut. 2021. [Analyzing commonsense emergence in few-shot knowledge models](#). In *Conference on Automated Knowledge Base Construction*.
- Damai Dai, Li Dong, Yaru Hao, Zhifang Sui, Baobao Chang, and Furu Wei. 2022. [Knowledge neurons in pretrained transformers](#). In *Proceedings of the 60th Annual Meeting of the Association for Computational Linguistics (Volume 1: Long Papers)*, pages 8493–8502, Dublin, Ireland. Association for Computational Linguistics.
- Javier De la Rosa, Eduardo G Ponferrada, Paulo Villegas, Pablo Gonzalez de Prado Salas, Manu Romero, and Maria Grandury. 2022. [BERTIN: Efficient pre-training of a spanish language model using perplexity sampling](#). *Procesamiento del Lenguaje Natural*, 68(0):13–23.
- Tim Dettmers, Artidoro Pagnoni, Ari Holtzman, and Luke Zettlemoyer. 2024. Qlora: Efficient finetuning of quantized llms. *Advances in Neural Information Processing Systems*, 36.
- Nelson Elhage, Tristan Hume, Catherine Olsson, Neel Nanda, Tom Henighan, Scott Johnston, Sheer ElShowk, Nicholas Joseph, Nova DasSarma, Ben Mann, et al. 2022a. Softmax linear units. *Transformer Circuits Thread*.
- Nelson Elhage, Tristan Hume, Catherine Olsson, Nicholas Schiefer, Tom Henighan, Shauna Kravec, Zac Hatfield-Dodds, Robert Lasenby, Dawn Drain, Carol Chen, et al. 2022b. Toy models of superposition. *arXiv preprint arXiv:2209.10652*.
- Nelson Elhage, Neel Nanda, Catherine Olsson, Tom Henighan, Nicholas Joseph, Ben Mann, Amanda

- Askell, Yuntao Bai, Anna Chen, Tom Conerly, et al. 2021. A mathematical framework for transformer circuits. *Transformer Circuits Thread*, 1:1.
- Javier Ferrando, Gerard I. Gállego, Ioannis Tsiamas, and Marta R. Costa-jussà. 2023. [Explaining how transformers use context to build predictions](#). In *Proceedings of the 61st Annual Meeting of the Association for Computational Linguistics (Volume 1: Long Papers)*, pages 5486–5513, Toronto, Canada. Association for Computational Linguistics.
- Leo Gao, Stella Biderman, Sid Black, Laurence Golding, Travis Hoppe, Charles Foster, Jason Phang, Horace He, Anish Thite, Noa Nabeshima, Shawn Presser, and Connor Leahy. 2020. The Pile: An 800gb dataset of diverse text for language modeling. *arXiv preprint arXiv:2101.00027*.
- Mor Geva, Avi Caciularu, Kevin Wang, and Yoav Goldberg. 2022. [Transformer feed-forward layers build predictions by promoting concepts in the vocabulary space](#). In *Proceedings of the 2022 Conference on Empirical Methods in Natural Language Processing*, pages 30–45, Abu Dhabi, United Arab Emirates. Association for Computational Linguistics.
- Mor Geva, Roei Schuster, Jonathan Berant, and Omer Levy. 2021. [Transformer feed-forward layers are key-value memories](#). In *Proceedings of the 2021 Conference on Empirical Methods in Natural Language Processing*, pages 5484–5495, Online and Punta Cana, Dominican Republic. Association for Computational Linguistics.
- Aitor Gonzalez-Agirre, Egoitz Laparra, and German Rigau. 2012. Multilingual central repository version 3.0: upgrading a very large lexical knowledge base. In *Proceedings of the 6th Global WordNet Conference (GWC 2012)*, Matsue.
- Stefan Heimersheim and Neel Nanda. 2024. How to use and interpret activation patching. *arXiv preprint arXiv:2404.15255*.
- G. E. Hinton, J. L. McClelland, and D. E. Rumelhart. 1986. *Distributed representations*, page 77–109. MIT Press, Cambridge, MA, USA.
- Graeme Hirst. 1987. *Semantic interpretation and the resolution of ambiguity*. Cambridge University Press.
- Edward J Hu, Yelong Shen, Phillip Wallis, Zeyuan Allen-Zhu, Yuanzhi Li, Shean Wang, Lu Wang, and Weizhu Chen. 2021. Lora: Low-rank adaptation of large language models. *arXiv preprint arXiv:2106.09685*.
- Ray S Jackendoff. 1992. *Semantic structures*, volume 18. MIT press.
- Robert Krzyzanowski, Connor Kissane, Arthur Conmy, and Neel Nanda. 2024. [We inspected every head in gpt-2 small using saes so you don't have to](#). Alignment Forum.
- Javier De la Rosa and Andres Fernández. 2022. Zero-shot reading comprehension and reasoning for spanish with BERTIN GPT-J-6B. In *Proceedings of the Iberian Languages Evaluation Forum (IberLEF 2022)*. CEUR Workshop Proceedings.
- Beth Levin. 1993. *English verb classes and alternations: A preliminary investigation*. University of Chicago press.
- Xiaopeng Li, Shasha Li, Shezheng Song, Jing Yang, Jun Ma, and Jie Yu. 2024. Pmet: Precise model editing in a transformer. In *Proceedings of the AAAI Conference on Artificial Intelligence*, volume 38, pages 18564–18572.
- Zhen Li, Xiting Wang, Weikai Yang, Jing Wu, Zhengyan Zhang, Zhiyuan Liu, Maosong Sun, Hui Zhang, and Shixia Liu. 2022. A unified understanding of deep nlp models for text classification. *IEEE Transactions on Visualization and Computer Graphics*, 28(12):4980–4994.
- Kevin Meng, David Bau, Alex Andonian, and Yonatan Belinkov. 2022. Locating and editing factual associations in gpt. *Advances in Neural Information Processing Systems*, 35:17359–17372.
- Kevin Meng, Arnab Sen Sharma, Alex Andonian, Yonatan Belinkov, and David Bau. 2023. Mass editing memory in a transformer. *The Eleventh International Conference on Learning Representations (ICLR)*.
- George A. Miller. 1994. [WordNet: A lexical database for English](#). In *Human Language Technology: Proceedings of a Workshop held at Plainsboro, New Jersey, March 8-11, 1994*.
- Neel Nanda. 2023. Attribution patching: Activation patching at industrial scale. URL: <https://www.neel-nanda.io/mechanistic-interpretability/attribution-patching>.
- Catherine Olsson, Nelson Elhage, Neel Nanda, Nicholas Joseph, Nova DasSarma, Tom Henighan, Ben Mann, Amanda Askell, Yuntao Bai, Anna Chen, et al. 2022. In-context learning and induction heads. *arXiv preprint arXiv:2209.11895*.
- OpenAI. 2023. Chatgpt. <https://chat.openai.com/>.
- Barbara Partee et al. 1984. Compositionality. *Varieties of formal semantics*, 3:281–311.
- Malka Rappaport Hovav and Beth Levin. 2008. The english dative alternation: The case for verb sensitivity. *Journal of linguistics*, 44(1):129–167.
- Gabriele Sarti, Nils Feldhus, Ludwig Sickert, and Oscar van der Wal. 2023. [Inseq: An interpretability toolkit for sequence generation models](#). In *Proceedings of the 61st Annual Meeting of the Association for Computational Linguistics (Volume 3: System Demonstrations)*, pages 421–435, Toronto, Canada. Association for Computational Linguistics.

Vivian Silva, Siegfried Handschuh, and André Freitas. 2016. *Categorization of semantic roles for dictionary definitions*. In *Proceedings of the 5th Workshop on Cognitive Aspects of the Lexicon (CogALex - V)*, pages 176–184, Osaka, Japan. The COLING 2016 Organizing Committee.

Paul Smolensky and Géraldine Legendre. 2006. *The harmonic mind: From neural computation to optimality-theoretic grammar (Cognitive architecture), Vol. 1*. MIT press.

Hugo Touvron, Louis Martin, Kevin Stone, Peter Albert, Amjad Almahairi, Yasmine Babaei, Nikolay Bashlykov, Soumya Batra, Prajwal Bhargava, Shrubhi Bhosale, et al. 2023. Llama 2: Open foundation and fine-tuned chat models. *arXiv preprint arXiv:2307.09288*.

Ashish Vaswani, Noam Shazeer, Niki Parmar, Jakob Uszkoreit, Llion Jones, Aidan N Gomez, Łukasz Kaiser, and Illia Polosukhin. 2017. Attention is all you need. *Advances in neural information processing systems*, 30.

Elena Voita, David Talbot, Fedor Moiseev, Rico Senrich, and Ivan Titov. 2019. Analyzing multi-head self-attention: Specialized heads do the heavy lifting, the rest can be pruned. *arXiv preprint arXiv:1905.09418*.

Ben Wang. 2021. Mesh-Transformer-JAX: Model-Parallel Implementation of Transformer Language Model with JAX. <https://github.com/kingoflolz/mesh-transformer-jax>.

Ben Wang and Aran Komatsuzaki. 2021. GPT-J-6B: A 6 Billion Parameter Autoregressive Language Model. <https://github.com/kingoflolz/mesh-transformer-jax>.

Kevin Wang, Alexandre Variengien, Arthur Conmy, Buck Shlegeris, and Jacob Steinhardt. 2022. Interpretability in the wild: a circuit for indirect object identification in gpt-2 small. *arXiv preprint arXiv:2211.00593*.

A Dataset Creation, Filtering, and Prompt selection

A.1 English WordNet (EWN)

The EWN dataset was constructed by selecting definienda consisting only of alphabetical letters and restricting the length of definitions to a maximum of 25 words to ensure computational efficiency. Samples were retained only if their definiendum matched a single item in the language model’s tokeniser vocabulary. This measure aimed to confine predictions to single-token inferences, thereby refining the precision and relevance of analytical outcomes. This process resulted in 8348 examples, with 80% allocated for training and 20% for testing.

A.2 Spanish WordNet (SWN)

For SWN, a procedure similar to that of creating the EWN was followed. Alphabetic words were chosen, and their definitions were searched in the Spanish WordNet. If found, they were selected, cleaned, and used. If not found, the Spanish word was translated to English, and its equivalent was searched in the English WordNet while matching their parts of speech. The English definition was then translated to Spanish using the Googletrans library, with back translation implemented to validate the translation’s correctness. This process resulted in 7815 examples in the Spanish dataset. We also limited the length of the accepted definitions to a maximum of 25 words, covering 99% of the samples.

A.3 Criteria and Process for Evaluating Prompts

When selecting prompts for evaluating the models on reverse dictionary definition generation, we prioritised testing clear prompts with real-world applicability, relevance to the task, and diversity in complexity. We included prompts with various linguistic structures, topics, difficulty levels, and additional information (metadata) added to the definition. As mentioned earlier in the paper, we continuously filtered the prompts to refine their clarity and effectiveness in guiding the models to the correct prediction. The prompts included direct ones such as: “Identify the term defined as: {definition}.” and “Provide the word corresponding to the definition: {definition}.”. We also tested prompts framed as questions, for example, “What word is described by this definition: {definition}?” and “For the given definition ‘{definition}’, what is the term?”. Prompts that naturally led to completing the definition with the definiendum were also utilised. Some examples include “{definition} is the definition of”, “{definition} is commonly known as”, and “{definition} is often referred to as:”. We also experimented with adding extra information to the prompts to see if that would improve the results. For example, adding the part of speech (POS) of the definiendum, as in “Identify the term defined as: {definition}, given the definiendum POS: {”}, or appending the POS for each word in the definition to the end of the prompt, as in “What

word is described by this definition: {definition}? given the definition POS: {}”. We found that simple, clear prompts without additional information about the predicted word yielded the best results, such as the prompt “{definition} is often referred to as:”.

B Annotation Overview for English Data

B.1 Definitional Semantic Roles (DSR) Overview

We describe each of the DSRs used in the paper in Table 1, following the definitions provided in (Silva et al., 2016).

Role	Definition
supertype	The superclass of the immediate entity or an ancestor of it
differentia quality	A fundamental, intrinsic attribute that sets the entity apart from others within the same supertype
differentia event	An action, state, or process in which the entity engages, necessary to differentiate it from others within the same supertype
event time	The time at which a differentia event occurs
event location	The specific location of a differentia event
quality modifier	A modifier indicating degree, frequency, or manner that refines a differentia quality
origin location	Specifies the entity’s place of origin
purpose	Defines the primary objective behind the entity’s existence or occurrence
associated fact	A fact connected to the entity’s existence or occurrence, serving as an incidental attribute
accessory determiner	A determiner expression that does not restrict the scope of supertype-differentia and can be omitted without altering the definition’s meaning
accessory quality	A non-essential attribute for characterising the entity
[role] particle	A particle, not contiguous with other role components

Table 1: Definition semantic roles and their definitions based on AST method.

C Models cards

We present model cards for the models utilised in this paper. Table 2 provides the hyperparameters of the GPT-J-6B model, while Table 3 presents the same for the fine-tuned BERTIN GPT-J-6B

model. GPT-J 6B is a large-scale autoregressive language model trained using Mech Transformer JAX (Wang, 2021), primarily on the text generation task using the Pile dataset (Gao et al., 2020) to learn English language representation. BERTIN-GPT-J-6B is a fine-tuned version of GPT-J 6B, trained on the mC4-es-sampled (gaussian) dataset (De la Rosa et al., 2022) also using Ben Wang’s Mesh Transformer JAX. Both models were fine-tuned for the reverse dictionary task by training them to predict a definiendum given a definition with a selected prompt (see Appendix A.3). The training process utilised LoRA (Hu et al., 2021), with the following settings: ‘10 epochs, batch size 16, r = 64, alpha 32, dropout 0.1’ for GPT-J-6B, and ‘20 epochs, batch size 16, r = 16, alpha 32, dropout 0.3’ for BERTIN-GPT-J-6B. The parameters underwent optimisations through iterative testing, leveraging LoRA with different settings tailored to enhance the performance of both GPT-J-6B and BERTIN-GPT-J-6B models in the reverse dictionary task. The parameters leading to the best performance were selected.

Hyperparameter	Value
$n_{\text{parameters}}$	6053381344
n_{layers}	28*
d_{model}	4096
d_{ff}	16384
n_{heads}	16
d_{head}	256
n_{ctx}	2048
n_{vocab}	50257/50400†(same tokenizer as GPT-2/3)
Positional Encoding	Rotary Position Embedding (RoPE)
RoPE Dimensions	64

Table 2: Hyperparameters of the GPT-J-6B model.

Hyperparameter	Value
$n_{\text{parameters}}$	6053381344
n_{layers}	28*
d_{model}	4096
d_{ff}	16384
n_{heads}	16
d_{head}	256
n_{ctx}	2048
n_{vocab}	50257/50400†(same tokenizer as GPT-2/3)
Positional Encoding	Rotary Position Embedding (RoPE)
RoPE Dimensions	64

Table 3: Hyperparameters of the BERTIN GPT-J-6B model.

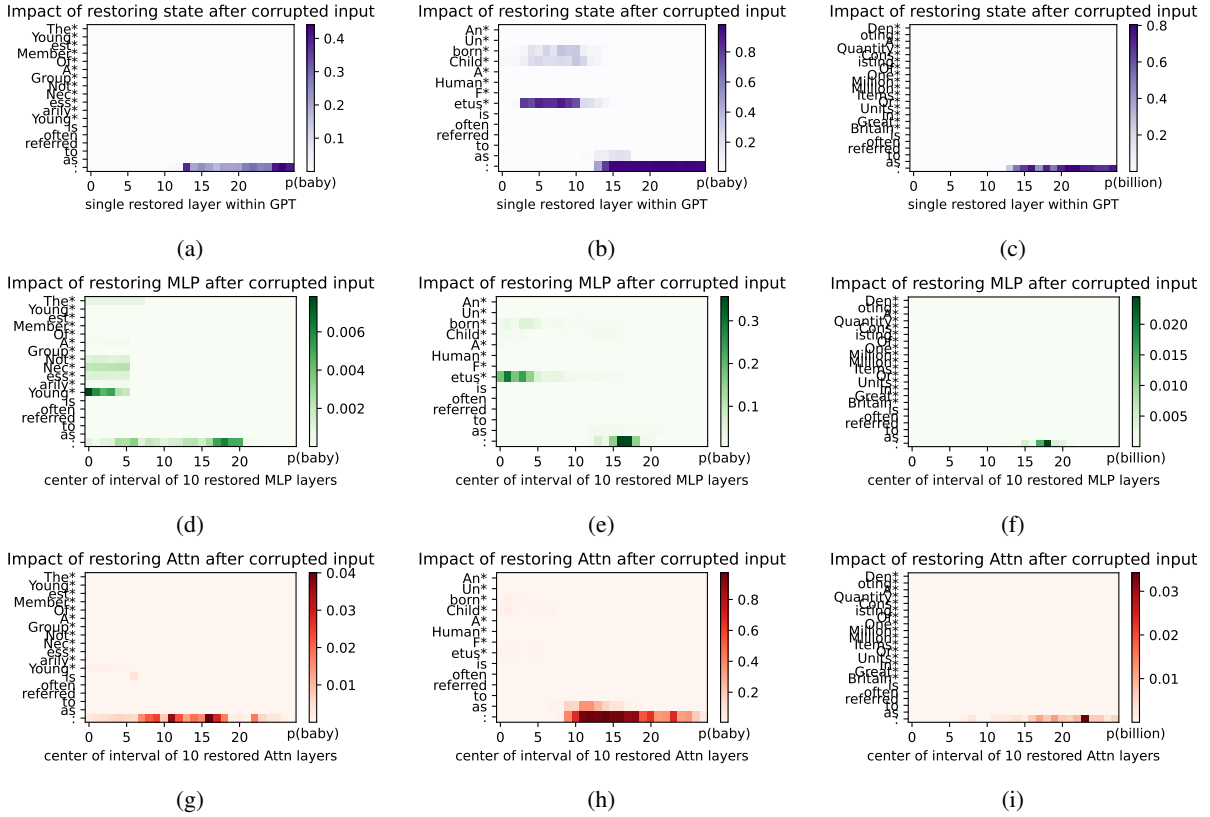


Figure 19: Causal traces for GPT-J-6B. These graphs demonstrate the impact of restoring a hidden state, a window of 10 MLP states and a window of 10 MHA states. Top row: Hidden states. Middle row: MLP states. Bottom row: MHA states.

D Supplementary results

D.1 Supplementary English results

The Figure 19 demonstrates additional results for the causal tracing. Figures 19a, 19b, 19d, 19e, 19g, and 19h show how the model handles homonyms based on the given definitions. For the hidden states (Figure 19b), all of its important states are concentrated with the last token, while in Figure 19a, other tokens are part of the critical states. The variation can be attributed to the second definition containing words highly linked to the definiendum, whereas the first does not. The same case can be observed with the MLP layers. Nevertheless, they tend to be more sensitive to words related to the term and use other tokens than the last one to make their decisions (Figure 19e). This suggests that they incorporate a broader context, are more sensitive, and rely on multiple tokens to determine the meaning of homonyms rather than focusing on the top layers’ representation. MHA layers maintain a consistent behaviour across the different cases (19g, and 19h), indicating their incline to generate a complete representation of the

input and passing it to the last token part of the input.

An example of number as token handling is also present (Figures 19c, 19f, 19g). In the hidden states and MHA, the model does not associate the decision with tokens containing other numerical values, such as “million”. Instead, it concentrates all of these important states with the last token, suggesting, as mentioned in the paper (Sections 4.2.3), that it deals with spelt-out numbers mainly as concepts rather than focusing on their arithmetic value. MLP layers behave similarly to the hidden states but with a shorter range of layers, further emphasising our hypotheses.

Finally, with all cases, the general patterns are consistent: hidden states aggregate a concept’s representation to the top layers and associate it with the last token, MLP layers utilise key tokens to generate input representations and recall the associated information with these representations in the middle layers, MHA layers apply compositionality to represent input and pick on semantic representation to generate and aggregate the representation in top layers.

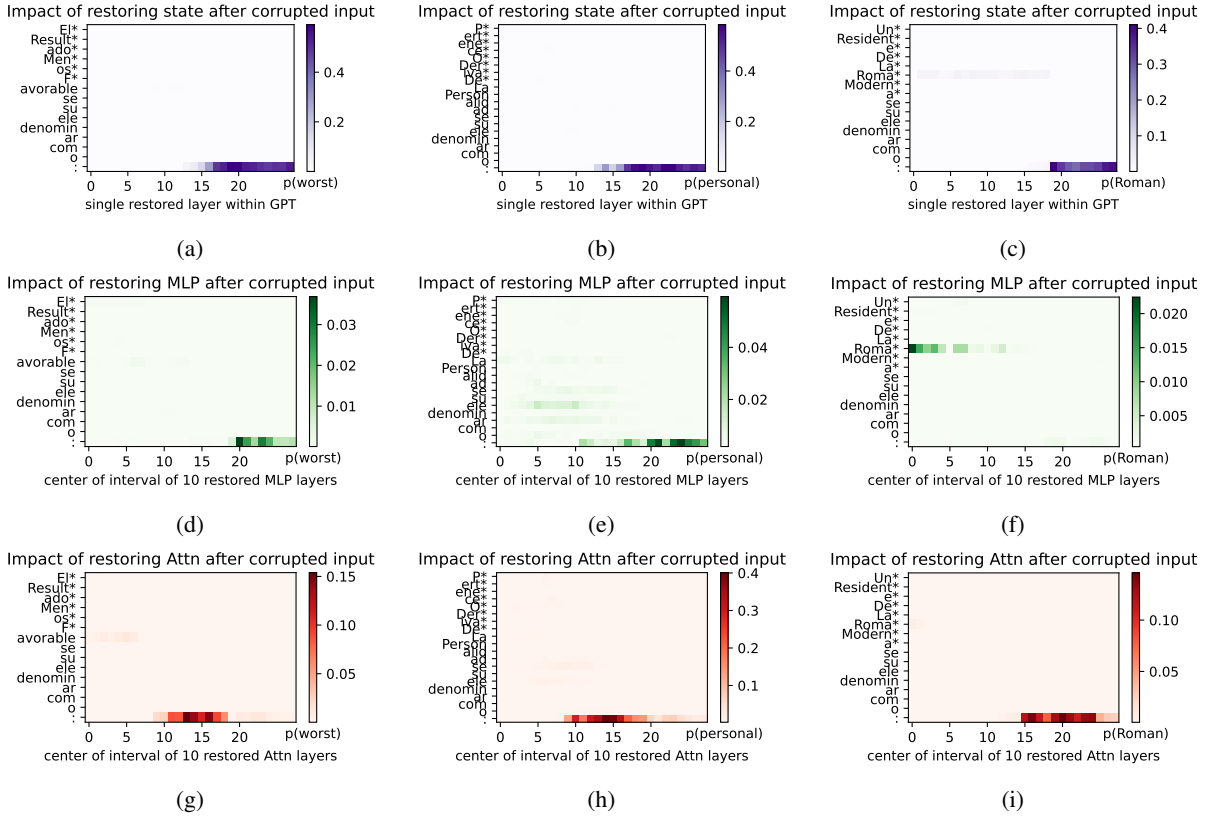


Figure 20: Causal traces for BERTIN GPT-J-6B. These graphs demonstrate the impact of restoring hidden, MLP, and MHA states. Top row: Hidden states. Middle row: MLP states. Bottom row: MHA states.

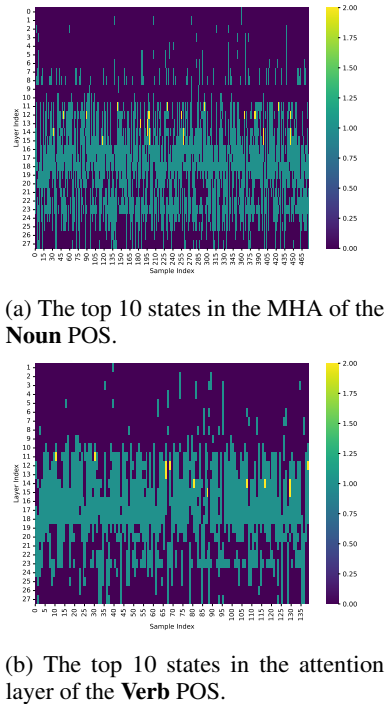


Figure 21: Sample of the top 10 states of the MLP and attention layer grouped based on POS of the definiendum.

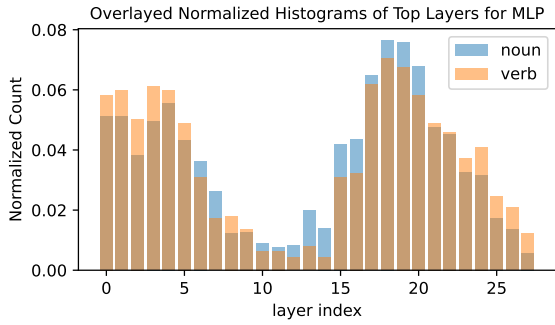
D.2 Supplementary Spanish results

Additional results for the causal tracing over the SWN are provided in Figure 20. The results of the Spanish data confirm our earlier findings from other states; the various components exhibit similar behaviour. The primary difference lies in the range of significant states, which appears to be more extensive. Detailed information can be found in Section 4.3.2.

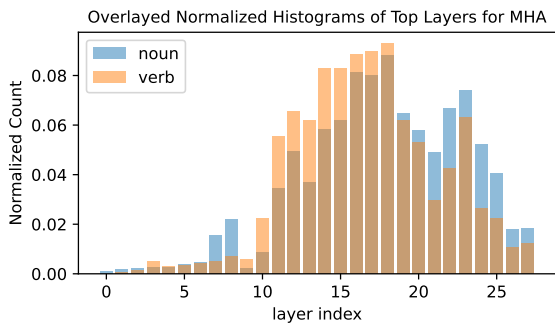
D.3 Grouping based on POS

Figure 21 additional results to grouping definitions based on the definiendum POS. It displays the top 10 states for the verb POS in the MLPs and MHA layers. As observed earlier in the paper (Section 4.2.1), when considering the POS of the definiendum, we notice little to no effect on the inference and behaviour of the model’s components.

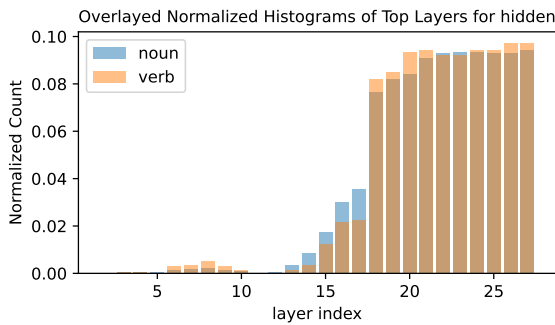
However, there are minor differences that can be inferred when we overlay the histograms of each group and component; we plot the distribution of top important states with this setting (Figure 22). In the MLP layers, the recall of nouns is slightly more concentrated at the top of the model compared to verbs (Figure 22a). In the MHA layers, the distri-



(a)



(b)



(c)

Figure 22: The top 10 states from (a) the MLP, (b) the MHA, and (c) the hidden layers, grouped based on the part of speech (POS) of the definiendum. The histogram of each component is overlaid and normalised.

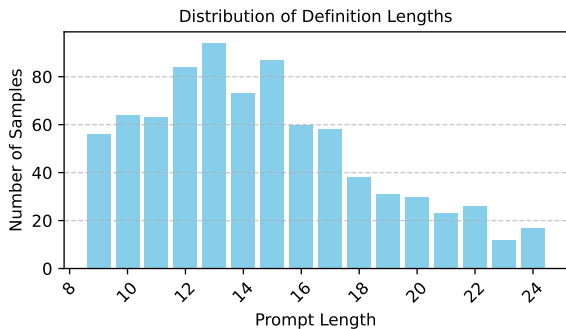


Figure 23: Distribution of Definition Lengths Across Samples.

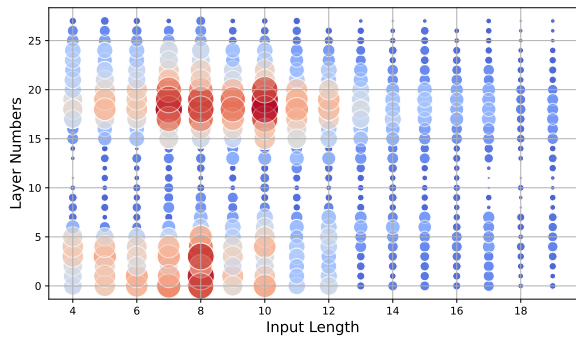
bution for verbs approximates a normal Gaussian shape, while that for nouns is slightly skewed (Figure 22b). Nevertheless, no clear differences can be discerned in the hidden layer (Figure 22c). Even though these differences are minor, they provide an indication of the distribution of information in LLMs. We hypothesise that this paves the way for exploring more methods of dividing the data or breaking it down into components, potentially leading to useful interpretability techniques.

D.4 Correlation with Definition Length

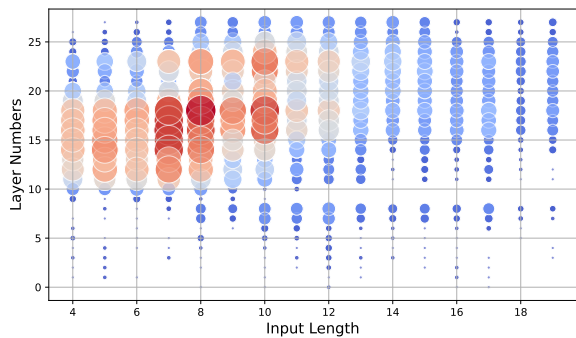
For completeness, the distribution of definition lengths across samples (Figure 23) is included to illustrate the sample sizes used for each. Also, the composite graph (Figure 24) visually summarises the results of MLP, MHA, and hidden state across various input lengths. Upon examination of the results, it was concluded that **there is no association between sentence length and the processes** used for hidden states, MLP layers, and MHA layers, further reinforcing the observation that the model’s internal mechanisms are well-equipped to handle varying input lengths without altering the fundamental processing approaches. The overall findings indicate a robust ability of the models to manage inputs of varying lengths by computing a representative vector for a concept and maintaining consistent processing strategies. This is clear in the consistent significance of the key tokens in the definition (e.g. Figures 3a and 3b), which also suggests that the compositional nature of inputs plays a significantly important role in achieving the necessary inference by models regardless of the context length.

E Experimental diagram

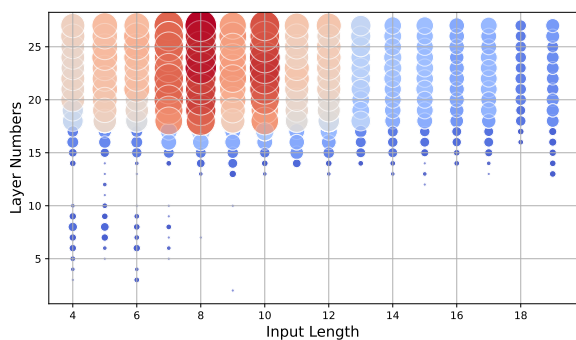
Figure 25 outlines the workflow for the empirical experiment, emphasising reproducibility and ease of understanding. It details each step and links to our research questions. Key components, such as references to relevant figures, tables, and results, are included.



(a) Distribution of Top Layer Numbers by Input Length in MLP (Concentration Highlighted).



(b) Distribution of Top Layer Numbers by Input Length in MHA (Concentration Highlighted).



(c) Distribution of Top Layer Numbers by Input Length in hidden (Concentration Highlighted).

Figure 24: The top 10 states from (a) the MLP, (b) the MHA, and (c) the hidden layers distributed based on the input length.

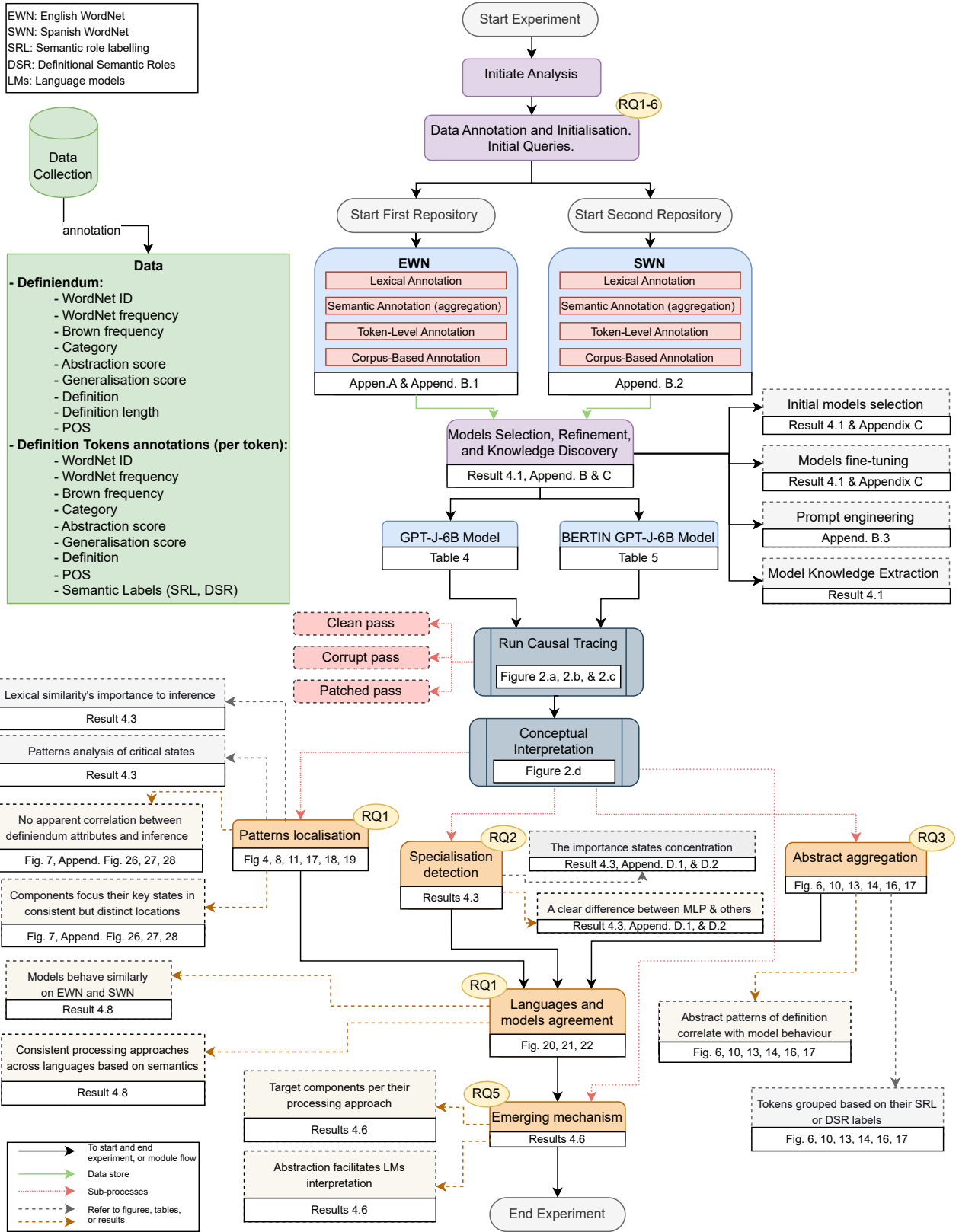


Figure 25: The workflow for the empirical experiment encompasses references to relevant figures, tables, and results.